RTO-TR-26
AC/323(AVT)TP/19

RTO-TR-26

NORTH ATLANTIC TREATY ORGANIZATION

RESEARCH AND TECHNOLOGY ORGANIZATION

BP 25, 7 RUE ANCELLE, F-92201 NEUILLY-SUR-SEINE CEDEX, FRANCE

© RTO/NATO 2000

Single copies of this publication or of a part of it may be made for individual use only. The approval of the RTA Information Policy Executive is required for more than one copy to be made or an extract included in another publication. Requests to do so should be sent to the address above.

RTO TECHNICAL REPORT 26

Verification and Validation Data for Computational Unsteady Aerodynamics

(Données de vérification et de validation pour l'aérodynamique instationnaire numérique)

Report of the Applied Vehicle Technology Panel (AVT) Task Group AVT-010.

Published October 2000

Distribution and Availability on Back Cover

5E. F-5 WING & F-5 WING + TIP STORE

Evert G.M. Geurts
National Aerospace Laboratory NLR, The Netherlands

INTRODUCTION

This data set relates to a transonic wind tunnel investigation carried out in 1977 on an oscillating, slightly modified model of the outer part of a Northrop F-5 wing with and without an external store. The store represented an AIM-9J missile including its launcher. These tests were reported in references 1, 2 and 3. The model proceeded from an F-5 wing model for subsonic tests by a slight reduction of the model span, needed to accommodate the tip store considered in the document. In streamwise direction the wing possesses a modified NACA 65-A-004.8 airfoil, characterised by a droopnose, extending from the leading edge towards the point of maximum thickness at 40 per cent of the chord.

The aim of the experiments was to determine the unsteady aerodynamic loads on a representative fighter type wing in the transonic and low supersonic speed regimes. Detailed steady and unsteady pressure distributions were measured over the wing, while on the store strain gauge balances obtained aerodynamic loads (Ref. 4). To study the effect of the external store on the unsteady wing loading (interference effects) as well as the unsteady loads on the store itself and its components, the model was tested in various stages of completeness. Starting with the clean wing, successively more parts of the store (launcher, missile body, aft wings, canard fins) were added. Data presented here refer accordingly to the F-5 clean wing configuration, growing in steps to the configuration of the F-5 wing with complete tip store. The model geometry described in the Formulary concerns only the clean wing; geometry data concerning the tip store are not described in this document. However, they are presented in the figures and they are contained in the database on the CD-ROM, accompanying this chapter. Simultaneously with these measurements also wind tunnel wall pressures were recorded to support wall interference effect studies. In the same test also various stages of an underwing missile were measured (pylon, launcher, missile body with aft wings, complete missile). However, no underwing missile data are included in this document.

Subsonic tests on the unmodified wing model in different tip store and underwing configurations were extensively reported in references 5 and 6. Tests on the same wing but with an inboard control surface were reported in reference 7.

The tests on the F-5 wing and F-5 wing with tip store were carried out in the High Speed Tunnel of the National Aerospace Laboratory NLR, in Amsterdam, The Netherlands. The tests covered the Mach number range between Ma = 0.6 and Ma = 1.35, and frequencies up to 40 Hz. An overview of the selected data is given in table 1. For steady measurements steady values are presented; for unsteady measurements mean values are represented as well as real and imaginary part of the unsteady values.

LIST OF SYMBOLS AND DEFINITIONS

Definition of axes systems

Figure 1 shows the body-fixed co-ordinate system used for non-dimensionalisation.

Figure 2 shows the body-fixed axis system (CATIA origin)

x-axis: chordwise co-ordinate in wing reference plane: apex: x = 0

y-axis: spanwise co-ordinate in wing reference plane; y-axis = rotation axis or pitching axis at $x/C_r = 50.00$ %

z-axis: co-ordinate in plane of symmetry normal to wing reference plane

Definitions of pressure, force and moment coefficients for the wing

Steady and mean

Pressure coefficient $$C_p = (P_{loc} - P) / Q$$

Sectional normal force $$C_z = Z / (Q * C) = -\int_0^1 (C_{p+} - C_{p-})\, d(x/C)$$

Sectional pitching moment about quarter-chord point (positive nose down) $$C_m = M / (Q * C^2) = -\int_0^1 (C_{p+} - C_{p-})\,(x/C - 0.25)\, d(x/C)$$

Unsteady

Pressure coefficient $$C_{pi} = \mathrm{Re}\, C_{pi} + i\, \mathrm{Im}\, C_{pi} = P_i / (Q * \theta)$$

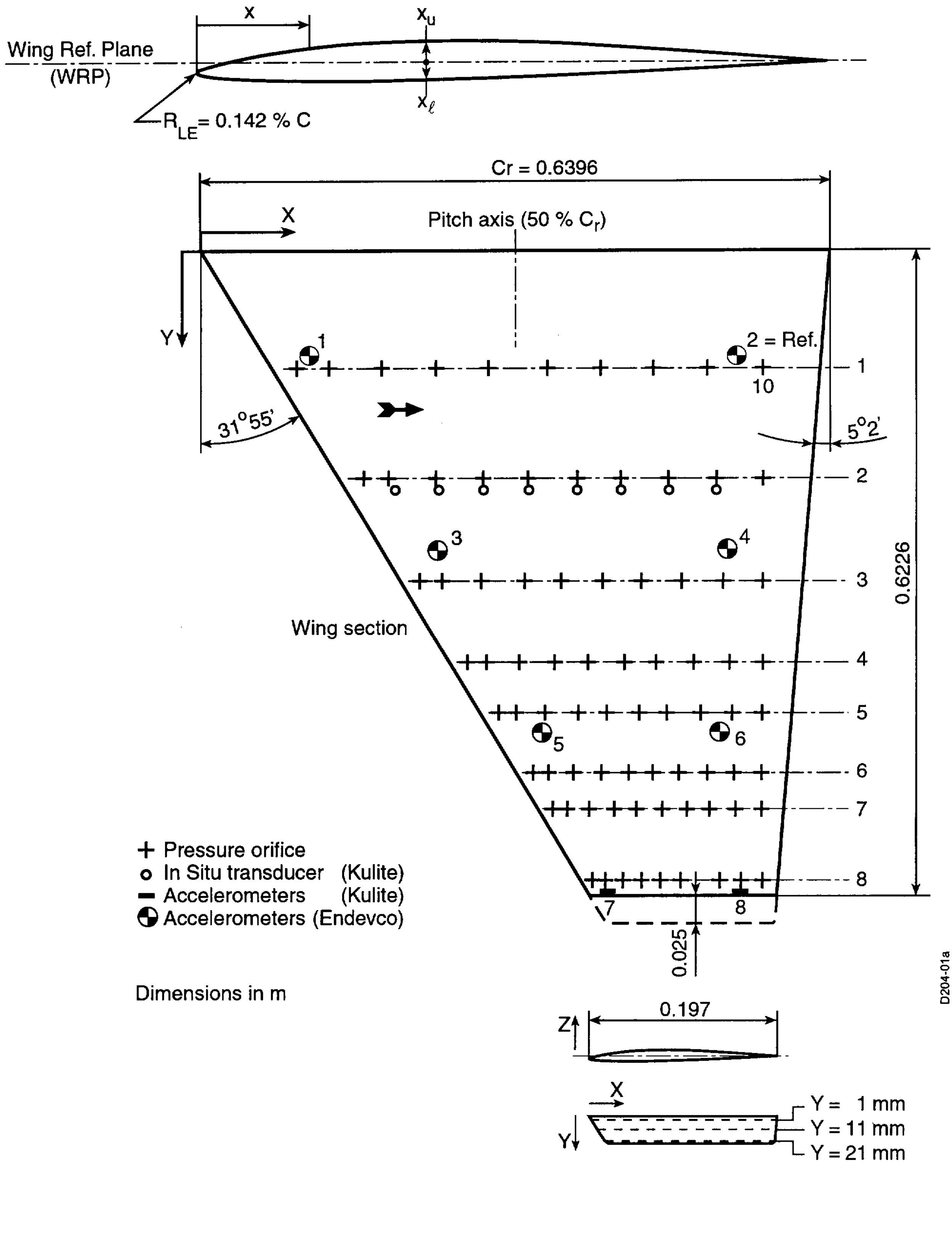

Figure 1: NLR F-5 clean wing, location of pressure orifices and transducers

4. F-5 CFD RESULTS

Michael J de C Henshaw
British Aerospace (Operations) Ltd.
Military Aircraft and Aerostructures,
Brough, East Riding of Yorkshire,
HU15 1EQ
UK
michael.henshaw@bae.co.uk

Stephane Guillemot
Dassault Aviation
78, Quai Marcel Dassault,
F-92214, Saint Cloud,
CEDEX
France
stephane.guillemot@dassault-aviation.fr

NOMENCLATURE

α	Angle of attack (deg.)
κ	Reduced frequency ($=\pi F C_r / V_\infty$)
θ	Maximum pitch angle (deg.)
η	Normalised spanwise co-ordinate (=y/s)
$\bar{c}$	Mean geometric chord (=0.4183m)
C_l	Lift coefficient
Cp	Pressure coefficient (See definitions in chapter 5.)
CpImag	Imaginary part of pressure coefficient for unsteady pressures (See definitions in chapter 5.)
CpReal	Real part of pressure coefficient for unsteady pressures (See definitions in chapter 5.)
C_r	Root chord (=0.6396 m)
F	Frequency of modal oscillation (Hz)
M	Mach number
Re	Reynold's number based on the mean geometric chord.
s	Span of wing
V_∞	Free-stream velocity (m/s)
y	Spanwise co-ordinate
Y+	Normalised wall distance of first cell height

INTRODUCTION

The F-5 test series (see chapter 5) provides a succession of geometries of increasing complexity [Ref. 1, Ref. 2], which will be useful for validating CFD codes during their development. In this chapter a range of CFD results are provided for the clean wing configuration at selected flow conditions, and a more limited set for one complex configuration. Results from essentially state of the art UTSP (Unsteady Transonic Small Perturbation), Full Potential, Euler, and NS (Navier-Stokes) codes are presented, this will allow the reader to gauge anticipated modelling accuracy for code development purposes. Table 1 summarises the methods used by contributors reported herein, the methods themselves are described in a standard pro-forma and the results collated as a series of plots. The flow conditions calculated are summarised in Table 2 and Table 4. Two or more methods are presented for each level of modelling approximation in order to assist the reader in gauging the likely level of variation in solution at a particular level of approximation.

Level of approximation	Contributor organisation	Method name/ identification label	Method type
UTSP	BAe.	UTSPV21	Cartesian/finite difference
UTSP	NASA	CAP-ASP	Cartesian/finite difference
Full Potential	CIRA	HELIFP	Structured/finite volume
Full Potential	Dassault Aviation	TCITRON	Structured/finite difference
Euler	INTA	EUL3DU	Structured/explicit/multiblock
Euler	Glasgow University	PMB3D	Structured multiblock/implicit
Euler	Dassault Aviation	EUGENIE	Unstructured finite volume / implicit
Euler	BAe.	UEMB	Structured/explicit/multiblock
Euler	NASA	ENS3DAE	Structured/finite difference
Navier-Stokes	NASA	ENS3DAE	Structured/finite difference

Table 1 CFD Methods

CFD SOLUTIONS

CLEAN WING TEST CASES

There are 14 cases (8 steady and 6 unsteady) as detailed in Table 2, in all cases the (equilibrium) angle of attack is close to zero, and the Mach number range includes sub-critical, transonic and supersonic flow conditions. Viscous effects are comparatively insignificant for these conditions.

Solutions are presented (on the CDROM) for upper and lower surfaces at 8 spanwise stations, as specified in Table 3 (see also figure 1 of chapter 5), and sample results are plotted at a few selected conditions and spanwise locations in this chapter. A selection of convergence plots is also provided.

The reader should note that the first data point on the upper surface for sections 3 and 5 are faulty pressure points (see Ref. 2) and should not be considered in evaluations. This can be observed in figures 5 to 10, particularly Figure 10.

Run No.	Mach No.	α (deg.)	freq. (Hz)	κ	θ (deg.)	Re X10^6
Steady cases						
137	0.597	-0.005	-	-	-	4.79
138	0.597	+0.493	-	-	-	4.77
151	0.897	-0.004	-	-	-	5.79
152	0.896	+0.497	-	-	-	5.79
158	0.946	-0.004	-	-	-	5.89
168	1.093	-0.002	-	-	-	6.01
190	1.328	-0.005	-	-	-	4.07
191	1.327	+0.500	-	-	-	4.08
Unsteady cases						
383	0.597	0.004	40	0.399	0.115	4.57
370	0.896	0.001	40	0.275	0.111	5.73
160	0.947	-0.006	20	0.132	0.523	5.91
373	1.092	0.003	10	0.058	0.113	5.92
172	1.093	0.003	20	0.116	0.267	6.02
193	1.336	-0.001	40	0.198	0.222	4.10

Table 2 Flow conditions used for comparisons

Section No.	η (=y/s)	y (m)
1	0.181	0.1127
2	0.352	0.2192
3	0.512	0.3188
4	0.641	0.3991
5	0.721	0.4489
6	0.817	0.5087
7	0.875	0.5448
8	0.977	0.6082

Table 3 Spanwise measurement stations on F-5 Wing.

a)

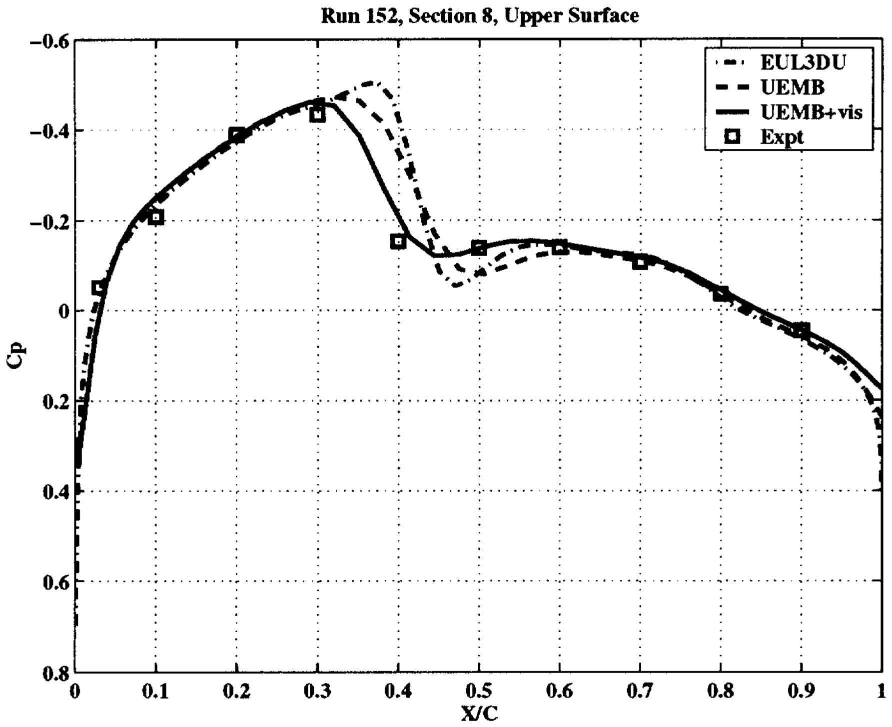

b)

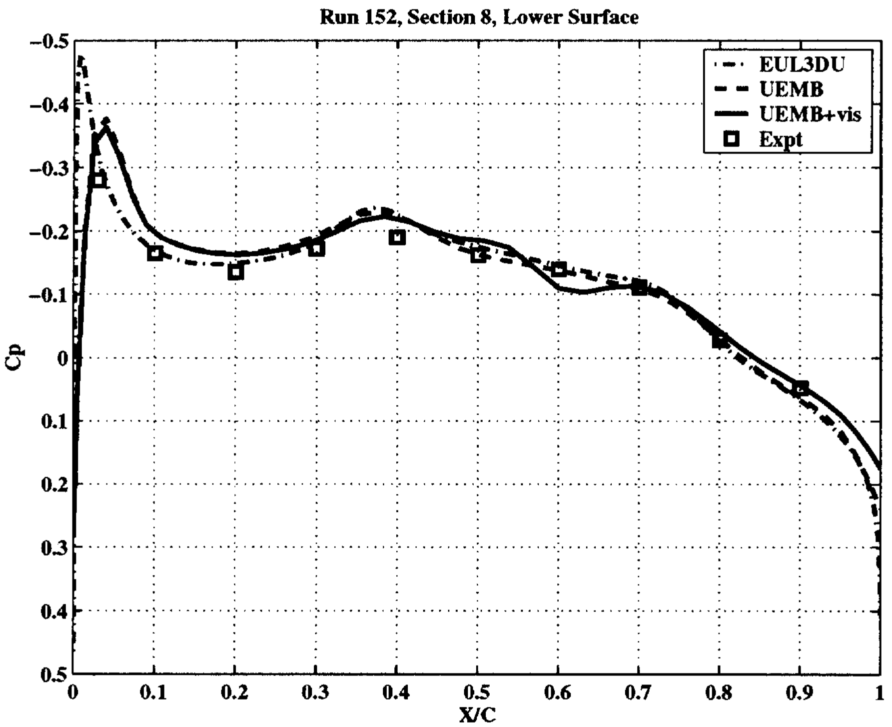

Figure 2 **Comparison of EUL3DU and UEMB at section 8 for run 152. Cp is plotted for a) upper surface, and b) lower surface. This figure shows that different tip modelling has less effect than other factors (such as inclusion of viscosity, designated UEMB+vis)**

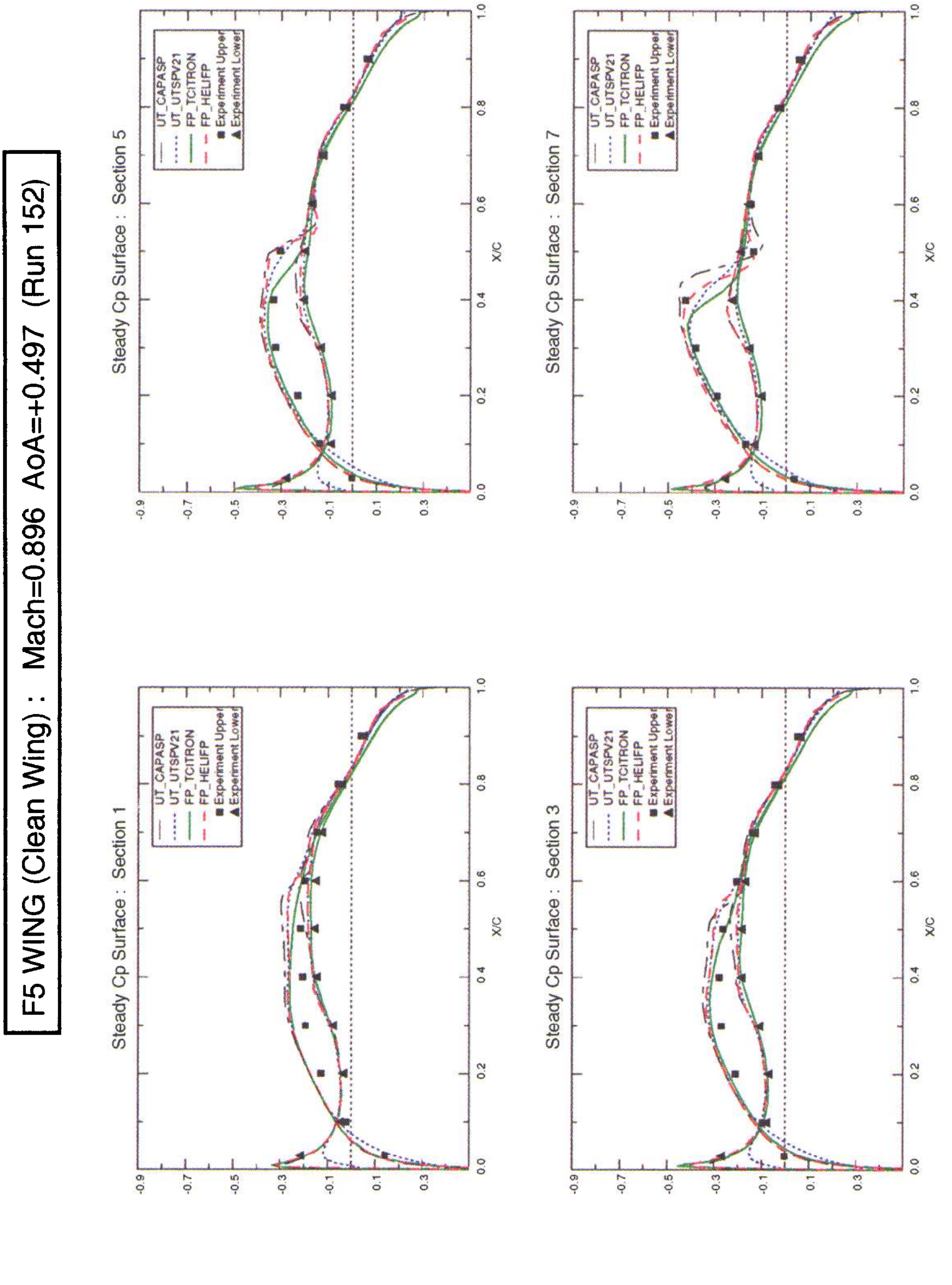

Figure 5 Code comparisons, steady flow. Run 152 (M=0.896, α=0.497°), Cp vs. X/C for UTSP and Full Potential codes (UTSPV21, CAP-ASP, TCITRON and HELIFP) at sections 1, 3, 5, and 7.